

Electronic spectroscopy of graphene obtained by ultrasonic dispersion

© A.G. Kastsova, N.V. Glebova, A.A. Nechitailov, A.O. Krasnova, A.O. Pelageikina, I.A. Eliseyev

Ioffe Institute, St. Petersburg, Russia

E-mail: glebova@mail.ioffe.ru

Received June 1, 2022

Revised October 14, 2022

Accepted October 24, 2022

A technology for obtaining graphene by means of ultrasonic dispersion of thermally expanded graphite in the presence of a surface-active polymer Nafion is presented. The technology makes it possible to obtain large amounts of low-layer (1–3 layers) graphene in a relatively short time. An approach to control the dispersion process based on UV spectroscopy of dispersions is described. A mechanism is proposed for the effect of a surface-active polymer on the production of low-layer graphene by ultrasonic dispersion.

Keywords: graphene, ultrasonic dispersion, thermally expanded graphite.

DOI: 10.21883/TPL.2022.12.54950.19268

In recent time, graphene has been increasingly used in various branches of technology due to such its properties as a unique (almost two-dimensional) structure [1], high electrical and thermal conductivities [2,3], high current carrier mobility [4], etc. There are publications devoted to employing its composites as materials for corrosion protection. Papers describe application of composites based on graphene and polymer Nafion [5], as well as of those based on graphene, boron nitride, and polyaniline [6]. In addition, graphene finds application as a catalyst carrier in electrochemical energy–conversion systems [7,8]. The role of graphene in improving thermal stability of the Nafion-type polymers is demonstrated [9].

As known, graphene is fabricated by chemically and mechanically induced cleavage of graphite layers. For instance, in work [10] there were studied graphene oxide (GO) obtained by the Hummers method and graphene reduced from the oxide. The paper reports that the obtained graphene contains several layers and exhibits in the Raman spectra an intense *D* line indicating the presence of defects that might be induced by the ultrasonic treatment. It is noticed that this fact may affect the graphene quality, which is one of the drawbacks of the procedure based on solutions. The authors note that further improvement of quality may be achieved by varying the solvent in the process of reduction.

The methodological and controlling aspects of the graphene production processes are important for obtaining and identification of materials with preset characteristics. Since the graphene materials (GO, various-layer graphene, graphene with different surface functional groups) possess characteristic electronic transitions, electron spectroscopy is a powerful tool for investigating these materials. Graphene is characterized by two peaks in the UV spectrum range: near 230 and 310 nm; these peaks correspond to transitions $\pi-\pi^*$ and $n-\pi^*$, respectively [10–13]. The $\pi-\pi^*$ absorption band is caused by conjugated bonds in the graphite hexagonal rings, while nonbonding electrons of functional groups of atoms (e.g. oxygen-containing ones)

are responsible for the $n-\pi^*$ absorption band. The peak positions on the wavelength axis depend on the factors affecting the electron energy states, namely, on the composition and number of functional groups and number of graphene layers, as well as, possibly, on the compounds adsorbed on the surface.

For instance, paper [10] has noticed that absorption spectra of the GO aqueous dispersion exhibit in the UV-visible range a peak at 235 nm which corresponds to the $\pi-\pi^*$ transition of sp^2 C=C bonds. This peak shifts towards a higher wavelength (265 nm) after the GO reduction to graphene. This effect is explained by an increase in the π -conjugation [11]. As the π -conjugation increases, the energy necessary for the transition decreases, which complies with the observed absorption shift towards higher wavelengths. Paper [12] shows that dispersions containing lowlayer (1–3 layers) GO can be distinguished from dispersions containing multilayer (4–10 layers) GO and GO with a higher number of layers (> 10) by the intense 230-nm peak in their UV-visible spectra. GO with 1–3 layers possesses a single peak, while GO with 4–10 layers has a weak shoulder-like peak. When the number of layers increases, the intensity of the multilayer GO shoulder tends to reduction. Neither the peak nor shoulder is observed for GO with a higher (> 10) number of layers. This observation made it possible to perform qualitative analysis of the GO dispersion. The results of X-ray photoelectron spectroscopy showed that variations in the intensity of the UV–visible light absorption in GO are caused by the conjugate effect associated with an increase in the number of chromophores (C–O, O=C, etc.) that affect the plasmon peak $\pi-\pi^*$.

In this work, we have studied a method for obtaining multilayer graphene by ultrasonic dispersion of thermally expanded graphite (TEG) in the presence of surfaceactive substances. As the initial material for dispersion, thermally expanded graphite was used [14]. The dispersion was performed in the isopropanol–water medium (with the volume ratio of 1:1) supplemented with perfluorinated sulfopolymer

Nafion (we used a commercial product, namely, a solution containing 20% of the polymer in the isopropanol–water mixture, Ion Power, Inc., DuPont DE2020).

Since the Nafion molecule contains hydrophobic (carbon skeleton $\cdots -CF_2-CF_2-$) and hydrophilic (sulfogroups $-SO_3H$) groups of atoms, the polymer possesses surface-active properties and, assumably, can be adsorbed on the surfaces of graphene layers (sheets). The polymer is expected to promote cleavage of graphite layers due to redistribution of density of π -electrons bounding them between formation of bonds with the polymer and spatial impact.

To prepare the initial mixture, the following precisely weighed portions of components were used: 1 mg of TEG, 14 mg 2% of the Nafion solution; 4 ml of the isopropanol + water (1:1) mixture were added. The mixture was exposed to ultrasonic treatment in the Branson 3510 UV bath at the power of ~ 180 W for ~ 180 min. After that, we took 2 droplets (0.04 ml) of the obtained suspension, added to them 4 ml of the isopropanol + water (1:1) mixture, and performed ultrasonic dispersion for different times.

In the process of dispersion, absorption spectra were recorded using a spectrophotometer Specord 210 with the rate of 1 nm/s and resolution of 1 nm. The spectra were measured in a quartz cell with the absorbing layer 1 cm long; as the reference solution, the isopropanol + water (1:1) mixture was used.

Studying the samples by Raman spectroscopy (RS) was performed at room temperature in the backscattering geometry using a multifunctional optical setup LabRAM HREvo UV-VIS-NIR-Open (HORIBA, France) equipped with a confocal optical microscope. As the laser radiation source, a 532nm laser Torus Nd:YAG (Laser Quantum, Inc., Great Britain) was used. The radiation power at the sample was $400 \mu\text{W}$ in the spot $1 \mu\text{m}$ in diameter.

Fig. 1 presents the TEG–dispersion absorption spectra recorded after dispersion for different times. The presented spectra enable making a number of conclusions. At the beginning of the dispersion (180 min), the spectrum exhibits in the shortwavelength range a shoulder with a very weakly pronounced maximum at 254 nm and a higherwavelength shoulder with a weakly pronounced maximum at ~ 312 nm. As the dispersion duration increases to 215 min, two well pronounced peaks corresponding to the $\pi-\pi^*$ (233 nm) and $n-\pi^*$ (312 nm) transitions appear in the spectrum. Further increase in the dispersion time to 245 min results in that the shortwavelength peak becomes more pronounced and shifts a little more to the shortwavelength range (228 nm). At the same time, the peak responsible for electron transition $n-\pi^*$ remains at the same place (~ 312 nm). Finally, after 305 min of dispersion both peaks do not change their positions, the only effect is that the shortwavelength (228 nm) peak becomes much more pronounced. Thus, analysis of the spectra dynamics evidences that TEG dispersion proceeds with formation of graphenes with different numbers of layers. The fact

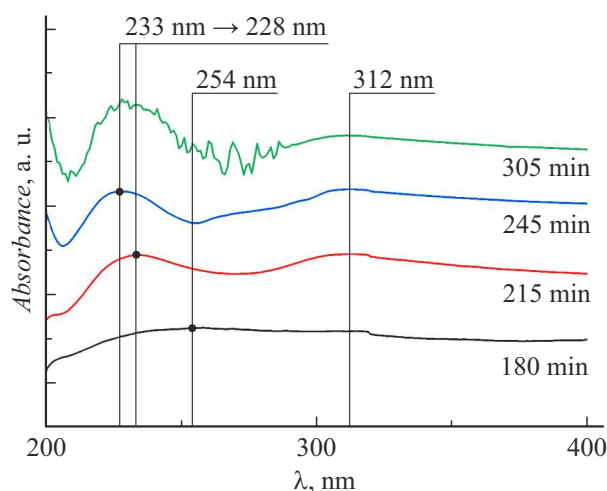


Figure 1. UV spectra of the TEG–Nafion dispersion in the isopropanol + water (1:1) mixture measured in the process of dispersion.

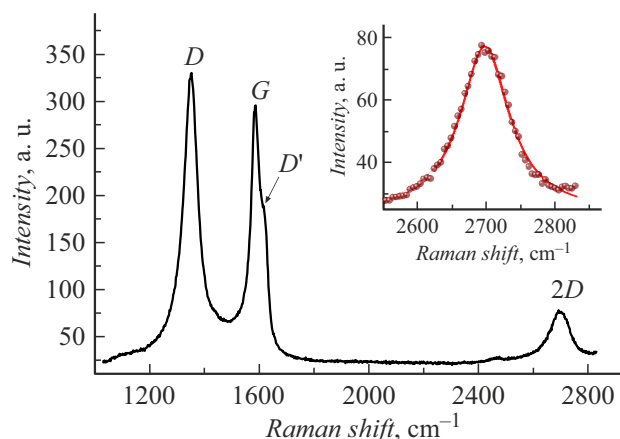


Figure 2. A Raman spectrum of a layer of the obtained graphene.

that the shortwavelength peaks become more pronounced evidences for a decrease in the number of layers during the dispersion down to 1–3 at the end of the process. To our mind, the shift of the shortwavelength peak position and relevant increase in the energy of electron transition $\pi-\pi^*$ (calculated via the known Planck's formula) from 4.88 eV at 180 min of dispersion to 5.32 and 5.44 eV at 215 and 245 min, respectively, demonstrate a decrease in the system energy (stabilization at a lower energy level) due to the polymer adsorption on the graphene surface. Notice that the electron transition energy dependence on the dispersion time reaches saturation and stops changing after 245 min of dispersion.

Fig. 2 demonstrates a Raman spectrum of the dispersed material film obtained by sputtering the dispersion on a silicon wafer with an aerograph.

The Raman spectrum exhibits three most significant clear lines: D , G and $2D$, and also line D' . The presence of intense line D , as well as of line D' , in the Raman spectrum

indicates a sufficiently high extent of the material defectiveness, which is characteristic of the fabrication technique used in this work. Data on the ratio between integral intensities of lines *D* and *G* ($A_D/A_G = 2.1$) and full width at half maximum of the *G* line ($\text{FWHM}(G) = 40 \text{ cm}^{-1}$) allows estimating the concentrations of onedimensional (crystallite boundaries) and 0dimensional (point) defects in graphene. Studies are available in which Raman spectra are used to estimate the typical size of crystallites and distance between twodimensional defects. In the framework of this approach, data of [15] shows that the mean size of crystallites in the sample is about 20 nm, while the mean distance between point defects is about 5 nm. Line 2*D* is well fittable to a single Lorenz function (the Fig. 2 inset), which is characteristic of graphene [16]. At the same time, the presence of defects in its crystal lattice makes line 2*D* rather broad ($\text{FWHM} \sim 90 \text{ cm}^{-1}$), which is characteristic of graphene about 2–3 monolayers thick. This agrees with the UV spectroscopy data given above.

The obtained results are of great interest for a wide range of applications in various fields. Our studies have provided data concerning a relatively simple and efficient technique for graphene fabrication and also an express–method for controlling its structure based on analyzing the UV spectra. A mechanism for dispersion using a surfaceactive polymer is proposed.

Conflict of interests

The authors declare that they have no conflict of interests.

References

- [1] A.K. Geim, *Science*, **324** (5934), 1530 (2009). DOI: 10.1126/science.1158877
- [2] K.S. Novoselov, A.K. Geim, S.V. Morozov, D. Jiang, Y. Zhang, S.V. Dubonos, I.V. Grigorieva, A.A. Firsov, *Science*, **306** (5696), 666 (2004). DOI: 10.1126/science.1102896
- [3] E.A. Yoo, J. Kim, E. Hosono, H.S. Zhou, T. Kudo, I. Honma, *Nano Lett.*, **8** (8), 2277 (2008). DOI: 10.1021/nl800957b
- [4] S. Stankovich, D.A. Dikin, G.H.B. Dommett, K.M. Rohlhaas, E.J. Zimney, E.A. Stach, R.D. Piner, S.T. Nguyen, R.S. Ruoff, *Nature*, **442**, 282 (2006). DOI: 10.1038/nature04969
- [5] J. Ding, P. Liu, M. Zhou, H. Yu, *ACS Sustain. Chem. Eng.*, **8** (40), 15344 (2020). DOI: 10.1021/acssuschemeng.0c05679
- [6] G. Tang, X. Hou, Y. Wang, Z. Yan, T. Ren, L. Ma, X. Huang, Ch. Wang, *ACS Appl. Nano Mater.*, **5** (1), 361 (2022). DOI: 10.1021/acsnm.1c03173
- [7] S.A. Grigoriev, V.N. Fateev, A.S. Pushkarev, I.V. Pushkareva, N.A. Ivanova, V.N. Kalinichenko, M.Yu. Presnyakov, X. Wei, *Materials*, **11** (8), 1405 (2018). DOI: 10.3390/ma11081405
- [8] I.V. Pushkareva, A.S. Pushkarev, M.A. Soloviev, V.N. Kalinichenko, R.G. Chumakov, Y. Liang, P. Millet, S.A. Grigoriev, *Catalysts*, **11** (2), 256 (2021). DOI: 10.3390/catal11020256
- [9] N.V. Glebova, A.A. Nechitailov, A.O. Krasnova, *Russ. J. Appl. Chem.*, **93** (7), 1034 (2020). DOI: 10.1134/S1070427220070137.
- [10] F.T. Johra, J. Lee, W. Jung, *J. Ind. Eng. Chem.*, **20** (5), 2883 (2014). DOI: 10.1016/j.jiec.2013.11.022
- [11] Y. Zhou, Q. Bao, L.A.L. Tang, Y. Zhong, K.P. Loh, *Chem. Mater.*, **21** (13), 2950 (2009). DOI: 10.1021/cm9006603
- [12] Q. Lai, Sh. Zhu, X. Luo, M. Zou, Sh. Huang, *AIP Adv.*, **2** (3), 032146 (2012). DOI: 10.1063/1.4747817
- [13] A.R. Baggio, M.S.C. Santos, F.H. Veiga-Souza, R.B. Nunes, P.E.N. Souza, S.N. Bao, A.O.T. Patrocinio, D.W. Bahnemann, L.P. Silva, M.J.A. Sales, L.G. Paterno, *J. Phys. Chem. A*, **122** (34), 6842 (2018). DOI: 10.1021/acs.jpca.8b05660
- [14] V.I. Mazin, E.V. Mazin, *Sposob polucheniya poristogo uglerodnogo materiala na osnove vysokorashcheplennogo grafita*, patent RF № 2581382 (publ. 20.04.2016). (in Russian)
- [15] L.G. Canado, M. Gomes da Silva, E.H. Martins Ferreira, F. Hof, K. Kamptoti, K. Huang, A. Penicaud, C.A. Achete, R.B. Capaz, A. Jorio, *2D Mater.*, **4** (2), 025039 (2017). DOI: 10.1088/2053-1583/aa5e77
- [16] A.C. Ferrari, J.C. Meyer, V. Scardaci, C. Casiraghi, M. Lazzeri, F. Mauri, S. Piscanec, D. Jiang, K.S. Novoselov, S. Roth, A.K. Geim, *Phys. Rev. Lett.*, **97** (18), 187401 (2006). DOI: 10.1103/PhysRevLett.97.187401